Journal of Photochemistry and Photobiology A: Chemistry 207 (2009) 306–310

Contents lists available at ScienceDirect

Journal of Photochemistry and Photobiology A: Chemistry

journal homepage: www.elsevier.com/locate/jphotochem

The sandwich structure electrodes based on wire-like TiO_2–β-cyclodextrin–SWCNT composite for dye-sensitized solar cells

Wei Zhou[a,b], Kai Pan[b], Chungui Tian[b], Yang Qu[b], Lili Zhang[b], Chia-Chung Sun[a,*], Honggang Fu[b,*]

[a] State Key Laboratory of Theoretical and Computation Chemistry, Jilin University, Changchun 130023, People's Republic of China
[b] Key Laboratory of Functional Inorganic Material Chemistry, Ministry of Education of the People's Republic of China, Heilongjiang University, Harbin 150080, People's Republic of China

ARTICLE INFO

Article history:
Received 25 November 2008
Received in revised form 17 July 2009
Accepted 28 July 2009
Available online 5 August 2009

Keywords:
Sandwich structure electrode
Composite
Dye-sensitized solar cells
Raman mapping

ABSTRACT

Wire-like TiO_2–β-cyclodextrin (CD)–SWCNT composites have been successfully fabricated through solar-induced self-assembly. The wires with the mean diameter of 1 μm were uniform and stable. β-CD molecules acted as linkers between SWCNT and monodisperse TiO_2 nanoparticles because β-CD can interact with both SWCNT and TiO_2 nanoparticles. The sandwich structure electrode based on the wires in the middle was fabricated. And the dye-sensitized solar cells with this sandwich structure electrode, which exhibited enhanced power conversion efficiency, were systematically studied. The improved photoelectrical performance was attributed to the effective separation of photoinduced electrons and holes and the rapid transportation of photogenerated electrons of SWCNT, which was demonstrated by surface photovoltage spectroscopy (SPS) and electrochemical impedance spectroscopy (EIS).

1. Introduction

Dye-sensitized solar cells (DSSCs) have attracted much attention because of their attractive features of high energy conversion efficiency and low production cost [1–6]. Typically, DSSCs are constructed by nanocrystalline semiconductor oxide photoelectrode, dye molecules, redox shuttle electrolytes and the counter electrode. And the photoelectrode is the main factor that determines the efficiency of DSSCs. Among nanocrystalline semiconductor oxide electrodes, TiO_2 has been one of the best choices for DSSCs due to its high dye adsorption and the fast electron transport, and has shown the high overall light conversion efficiency over 11% [7]. But the primary weakness of the small electron diffusion coefficient limits the random walk of electrons through the nanoparticle film [8]. One strategy for reducing the dimensionality of the network in order to make electron transport faster has been widely adopted [9–13]. However, the low surface area of one-dimensional photoelectrode materials determined their low dye adsorption, which resulted in the lower efficiency compared to nanoparticle films. Therefore, it is necessary to synthesize new low-dimensional composites with high dye adsorption and fast electron transport in order to enhance the efficiency of DSSCs.

Due to the unique electronic, mechanical, and chemical properties of carbon nanotubes (CNTs), TiO_2-CNTs hybrid is a promising material among many composites because it possesses the merit of the building blocks, i.e. high dye adsorption of TiO_2 and fast electron transport of CNTs [14–17]. However, the interfacial charge-transfer was not improved effectively because of the incompact structure. Therefore, a further improvement of the TiO_2–CNTs interface is still a great challenge. Based on the works of wire-like cyclodextrin (CD)–TiO_2 composites and single wall carbon nanotube (SWCNT)–CD composites, it is possible to fabricate wire-like TiO_2–CD–SWCNT composite, because CD can interact with both SWCNT and TiO_2 nanoparticles.

On the basis of the above consideration, combining the self-assembly behavior of β-CD, and its interaction with TiO_2 nanoparticles and SWCNT, we design and fabricate a novel wire-like TiO_2–β-CD–SWCNT composite through solar-induced self-assembly of monodisperse TiO_2 nanoparticles and SWCNT–β-CD composites. The compact composite structure of TiO_2–β-CD–SWCNT offers possibility to increase the separation and transportation of photogenerated charges. So, we design a sandwich structure electrode including this wire-like TiO_2–β-CD–SWCNT composite in the middle in DSSCs and it exhibits enhanced power conversion efficiency. This is because the compact

* Corresponding authors. Tel.: +86 451 8660 8458; fax: +86 451 8667 3647.
E-mail addresses: huangxr@mail.jlu.edu.cn, fuhg@vip.sina.com (H. Fu).

1010-6030/$ – see front matter © 2009 Elsevier B.V. All rights reserved.
doi:10.1016/j.jphotochem.2009.07.029

composite structure of TiO_2–β-CD–SWCNT wire and the unique electronic property of SWCNT are in favor of the transportation of photogenerated electrons in this sandwich structure.

2. Experimental

2.1. Synthesis

The details for synthesis of SWCNT–β-CD composites [18], and monodisperse TiO_2 nanoparticles [19] were given elsewhere. Typically, 1 mg TiO_2 and 5 mg SWCNT–β-CD were mixed with 1 mL distilled water and then sonicated for 5 min. The pH of the suspension was about 7. After irradiating under solar at room temperature for 3 weeks, wire-like composites were observed. These wires were separated and washed with distilled water completely. The wires were very stable for more than several months. Control experiment of UV irradiation with a 20 W UV lamp was made and similar results were observed, the growth of wire-like composites could be easily controlled by adjusting the intensity of UV irradiation.

2.2. Characterization

Scanning electron microscopy (SEM) micrographs were taken using a Philips XL-30-ESEM-FEG instrument operating at 20 kV and S-4800 Hitachi at 15 kV, High-Technologies Corporation, respectively. Raman measurements were performed with Jobin Yvon HR 800 micro-Raman spectrometer at 457.9 nm. The Raman mapping was obtained by focusing the laser beam with 50× magnification. The surface photovoltage spectroscopy (SPS) measurement was carried out with a home-built apparatus which was described elsewhere [20]. The electrochemical impedance spectroscopy (EIS) was performed with a computer-controlled IM6e Impedance measurement unit (Zahner Elektrik, Germany). EIS was obtained by applying sinusoidal perturbations of 10 mV over the V_{oc} at the frequency range from 0.05 to 100 kHz. All EIS measurements were carried out under illumination of 10 mW cm^{-2}. The obtained spectra were fitted with ZsimpWin software in terms of appropriate equivalent circuits.

2.3. Photoelectrochemical measurements

The sandwich structure electrode was prepared as follows. The first layer of the TiO_2 film was prepared by a doctor-blade method on the FTO (F-doped SnO_2 layer, sheet resistance is 20 Ω/square) substrate [21]. TiO_2 paste was obtained by homogeneously mixing 2 mL ethanol and 680 mg TiO_2 (Degussa P25). The longer FTO edges were covered with transparent adhesive tape to control the film thickness and 0.1 mL of the paste was spread over the surface, and then sintered at 450 °C for 30 min. The middle layer, which was also prepared by a doctor-blade method, was obtained by homogenously mixing 1 mL distilled water and 1 mg TiO_2–β-CD–SWCNT composites. The third layer of the TiO_2 was prepared by a doctor-blade method too. This sandwich structure film was finally pressed at 1000 kg cm^{-2} between stainless-steel plates in a hydraulic press [22]. This electrode was designated as A. As a control, the sandwich electrode with the middle layer of SWCNT which was prepared by electrophoretic deposition method between two layers TiO_2 nanoparticle was fabricated [23], deposition voltage and time were 100 V and 2 min, respectively, denoted as B. The electrode with only two layer TiO_2 nanoparticle thin films was also prepared, designated as C. The thicknesses of all three samples were around 15 μm.

The films were immersed in 0.5 mM $(C_4H_9)_4N)_2$[Ru-(4-carboxy-4′-carboxylate-2,2′-bipyridine)$_2$$(NCS)_2$] dye (N719, Solaronix SA, Switzerland) in acetonitrile and tert-butanol (volume ratio, 1:1) for 12 h. Platinum counter electrodes were prepared following literature [7]. The dye-sensitized electrodes and Pt counter electrode were cohered together with epoxy resin. The electrolyte that was composed of 0.6 M 1-propyl-2,3-dimethylimidazodiumiodide, 0.05 M I_2, 0.1 M LiI, and 0.5 M tert-butylpyridine in 3-methoxypropionitrile was admitted by capillary action. The DSSCs assembled with A, B, and C were designated as Cell A, B, and C, respectively. Photocurrent and photovoltage were recorded by BAS100B Electrochemical Analyzer. A 400 W xenon lamp with UV filter was used as a light source. Its intensity was about 40 mW cm^{-2}. The irradiation area was about 0.12 cm^2. After testing, desorption experiment was performed to determine the amount of dye adsorption as follows. The dye-sensitized electrodes were immersed in 0.02 M NaOH solution in alcohol (EtOH) and H_2O (volume ratio, 1:1) for 6 h.

3. Results and discussion

3.1. Structure and morphology of wire-like TiO_2–β-CD–SWCNT composites

Under solar irradiation, wire-like TiO_2–β-CD–SWCNT composite was formed. SEM images of wire-like TiO_2–β-CD–SWCNT composites are shown in Fig. 1. It can be clearly seen that the wires with the mean diameter of about 1 μm were long and uniform (Fig. 1A). Amplified SEM image of the wire shown in the inset of Fig. 1A indicates monodisperse TiO_2 particles cover on the surface of the wire uniformly. Control experiments under UV irradiation are also made and the result is similar to that of solar irradiation (Fig. 1B).

Raman measurements were used to investigate the distribution of monodisperse TiO_2 nanoparticles and SWCNT in this wire. Fig. 2

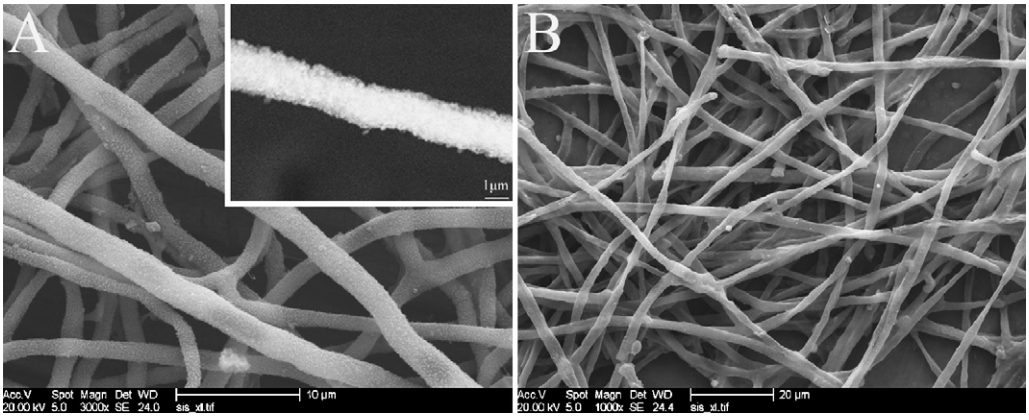

Fig. 1. Representative SEM images of wire-like TiO_2–β-CD–SWCNT composites (A: solar irradiation; B: UV irradiation).

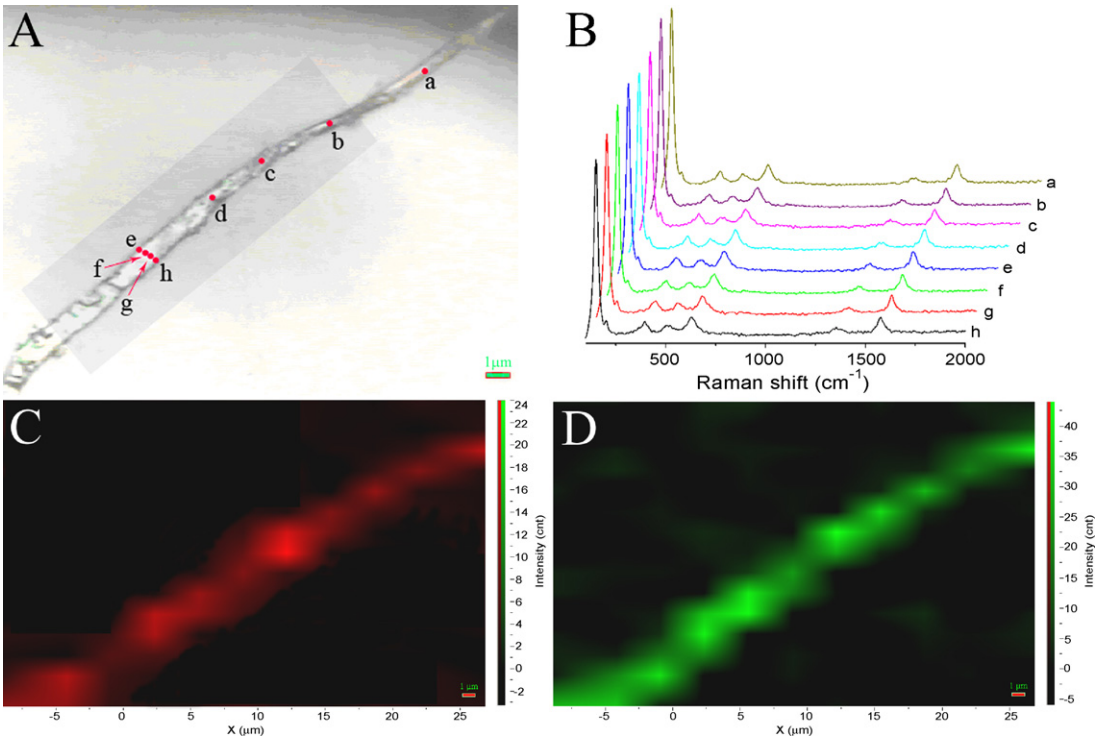

Fig. 2. Light microscopy image of wire-like TiO_2–β-CD–SWCNT composite (A) and its corresponding Raman spectra (B) and the Raman mapping of the defined area (C: TiO_2; D: SWCNT).

shows the image of a single wire-like TiO_2–β-CD–SWCNT composite under solar irradiation and its corresponding Raman spectra and Raman mapping. The points of a, b, c, d, and e, f, g, h, are longitudinal and lateral distribution of the wire, respectively (Fig. 2A). From Fig. 2B, the peaks at 148, 199, 393, 513, and 638 cm^{-1} can be ascribed to E_g, E_g, B_{1g}, A_{1g} (B_{1g}), and E_g modes, respectively, which are the characteristics of anatase TiO_2 [24]. Meanwhile, the characteristic D-band at 1361 cm^{-1} and G-band at 1580 cm^{-1} of SWCNT (Fig. 2B), corresponding to the disordered mode and tangential mode [25], respectively, could be clearly observed, indicating the existence of SWCNT. Raman mapping of the defined area of a single wire is shown in Fig. 2C and D. It shows the distribution of E_g (149 cm^{-1}) mode of monodisperse TiO_2 nanoparticles (Fig. 2C) and D-band (1361 cm^{-1}) of SWCNT (Fig. 2D), respectively. Obviously, monodisperse TiO_2 nanoparticles and SWCNT distribute uniformly along the wire. The formation of wire-like TiO_2–β-CD–SWCNT composite proves that β-CD molecules acted as linkers between SWCNT and monodisperse TiO_2 nanoparticles. From Raman and Raman mapping analysis, we can reveal that monodisperse TiO_2 nanoparticles and SWCNT distribute homogeneously in this wire.

3.2. Photoelectrochemical property and analysis

Generally, the rapid electron transport is important to ensure their efficient collection in DSSCs. In TiO_2 nanoparticle film, the electron transport across nanoparticles is easy for recombination loss at the grain boundaries [26]. Fabrication of films from one-dimensional structures has been proven to be an effective way to facilitate electron transport [9,27,28]. In order to obtain rapid electron transport and high roughness factor similar to TiO_2 nanoparticles, we design the sandwich structure electrode to improve the efficiency in DSSCs. Fig. 3 shows the schematic representation of the sandwich structure electrode. We can clearly understand the sandwich structure from this scheme. The SEM images of cross-sections for electrodes A (a), B (b) and C (c), respectively, were shown in Supplementary Data (Figure S1). The

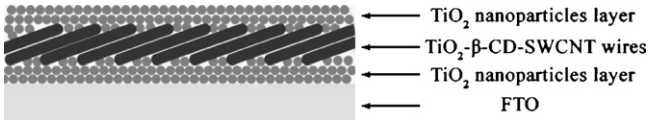

Fig. 3. The schematic representation of the sandwich structure electrode.

thicknesses of the three samples were similar and all around 15 μm. From Figure S1a we can clearly see that the TiO_2–β-CD–SWCNT wires layer was between two TiO_2 nanoparticles layers. Therefore, the TiO_2–β-CD–SWCNT wires acted as linkers between two TiO_2 nanoparticles layers. However, the SWCNT layer was not observed obviously (Figure S1b). That is because the diameter of SWCNT was only about 2 nm, they could not be observed clearly at this large scale. Therefore, the image of the sandwich structure electrode could be presented clearly by the SEM images of cross-sections.

The photocurrent and photovoltage characteristics and the working parameters of each solar cell consisting of Cell A, B, and C, respectively, are summarized in Table 1. Each value for cell performance was taken as an average of at least four samples. It can be seen that the short-circuit current density (J_{sc}) and power conversion efficiency (η) of Cell A (7.7%) was higher than that of Cell B (7.3%) and C (7.2%). Owing to the incorporation of wires, especially, the film thickness of the three electrodes are the same, that is to say, the wires replace some TiO_2 particles, so the roughness factor of Cell A may be slightly lower than Cell C. Accordingly, the dye loading of

Table 1
Comparison of device performance parameters for this film in a DSSCs environment.

Cell	J_{sc} (mA/cm^2)	V_{oc} (V)	FF	η (%)
Cell A	6.54	0.649	0.72	7.7
Cell B	6.29	0.632	0.72	7.3
Cell C	6.25	0.636	0.72	7.2

Note. J_{sc}: short-circuit photocurrent; V_{oc}: open-circuit photovoltage; FF: fill factor; η: power conversion efficiency.

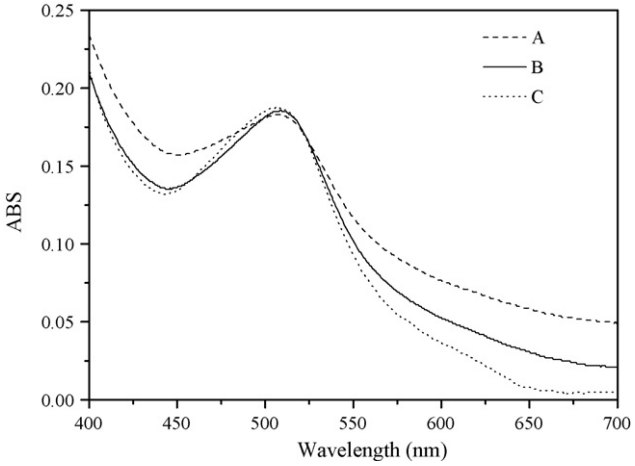

Fig. 4. The UV–visible absorption spectra of desorption N719 dye from Cell A, B and C, respectively.

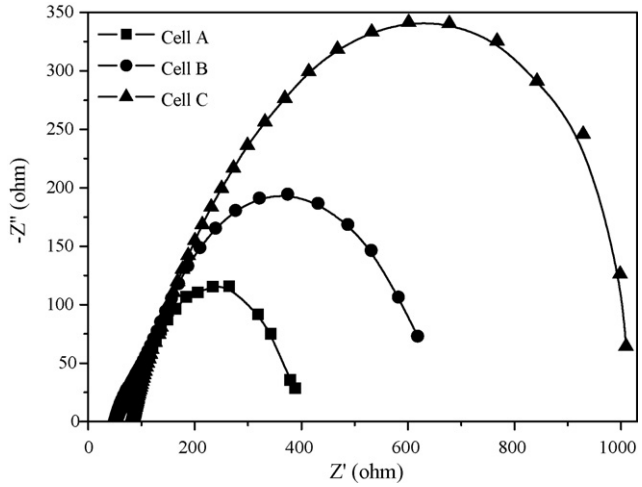

Fig. 6. Electrochemical impedance spectroscopy (EIS) Nynquist plots of Cell A, B and C, respectively.

them may be different. In order to investigate the dye loading of the three cells, UV–visible absorption measurement was performed. Fig. 4 shows the UV–visible spectra of Cell A, B and C after desorption in NaOH solution, respectively. According to Beer–Lambert law, the molar concentration of dye loading from Cell A, B, and C was 1.30×10^{-5}, 1.31×10^{-5}, and 1.32×10^{-5} mol L^{-1}, respectively [29]. That is to say, dye loading of the three cells changed slightly. Therefore, the main reason for the higher current density should not come from dye loading.

According to the analysis above, we speculate the enhanced J_{sc} can be ascribed to the rapid electron transport rate through wires which possess of the compact composite structure. In order to confirm this hypothesis, surface photovoltage spectroscopy (SPS) was performed. SPS is a proper tool to investigate the photophysical processes of semiconductor, such as charge-transfer and separation [20,30,31]. Fig. 5 shows the SPS responses of A, B, and C, respectively. For all samples, a SPS response at around 345 nm is found. This is attributed to electron transitions from the valence to conduction band (band-to-band transitions, O_{2p}–Ti_{3d}) [20,32,33]. Compared with B and C, A has the strongest SPS response, indicating that its separated efficiency of photogenerated charges is the highest [34]. It confirms that photoinduced electron–hole pairs are easily separated and the electrons transfer rapidly in this wire. It is very interesting to note that the SPS response of A (347 nm) is red-shifted compared with that of C (342 nm). This is attributed to the introduction of the wires including SWCNT. It is reported that the apparent Fermi level was positively shifted in TiO_2–CNTs composites, which was an indication of the electron transfer from TiO_2 to CNTs as the two systems undergo charge equilibration [17,35,36]. The equilibration of electrons between SWCNT and TiO_2 results in the transfer of parts of electrons into SWCNT, thus stabilizing the photogenerated electrons and reducing the rate of recombination. Therefore, the positively shift of the apparent Fermi level was the main reason for the red-shift of the SPS responses. Accordingly, the introduction of the wires, especially the compact composite structure favors of the rapid electrons transportation and reducing the recombination, is the main reason for the enhanced efficiency of Cell A.

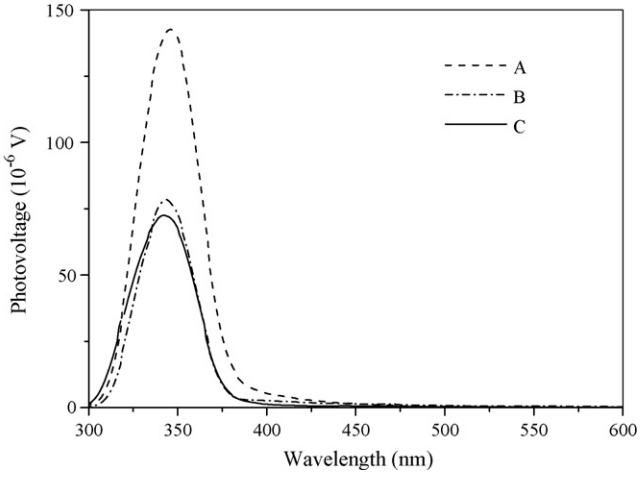

Fig. 5. The surface photovoltage spectroscopy (SPS) responses of A, B, and C, respectively.

Electrochemical impedance spectroscopy (EIS) is one of powerful methods to investigate internal resistances that is attributed to charge-transfer process of DSSCs. Fig. 6 shows EIS Nynquist plots of Cell A, B and C, respectively. The diameter of the arc radius on the EIS Nynquist plot of Cell A is smaller than that of Cell B and Cell C obviously. From the Nynquist diagram, the obtained resistances values for Cell A, B and C are 102.8, 113.1 and 511.2 Ω, respectively. The smaller the arc radius is, the higher the efficiency of charge separation is [37,38]. The EIS data better explain the fast charge transport in this sandwich structure electrode. Therefore, in the case of Cell A, the photoinduced electron–hole pairs are easily separated and transferred to conductive substrate which is due to the introduction of the wires including SWCNT. Thus, the photoinduced electrons and holes are separated more efficiently in Cell A because of the compact composite structure of TiO_2–β-CD–SWCNT. This is in good agreement with the SPS results. Therefore, the enhanced efficiency can attribute to the unique electronic property of SWCNT and the compact composite structure of TiO_2–β-CD–SWCNT in this structure in favor of the rapid transportation of photogenerated electrons, subsequently reduced recombination.

4. Conclusions

In summary, wire-like TiO_2–β-CD–SWCNT composites have been successfully fabricated by solar-induced self-assembly. The wires were long and uniform. The analytical results confirmed that monodisperse TiO_2 nanoparticles and SWCNT distributed uniformly in this wire. β-CD molecules acted as linkers between SWCNT and monodisperse TiO_2 nanoparticles. Moreover, the sandwich structure electrode containing the wires in the middle

exhibited the 7% enhanced efficiency in DSSCs. The SPS and EIS investigation confirm that the effective separation of photoinduced electrons and holes and the rapid electrons transportation of the compact structure of TiO_2–β-CD–SWCNT are the main reasons for the high efficiency. This sandwich structure electrode including one-dimensional materials represents a promising approach for further improving the efficiency in DSSCs.

Acknowledgements

This work was supported by the Key Program Projects of National Natural Science Foundation of China (no. 20431030), the National Natural Science Foundation of China (no. 20671032), and the Key Program Projects of the Province Natural Science Foundation of Heilongjiang Province (no. ZJG0602-01).

Appendix A. Supplementary data

Supplementary data associated with this article can be found, in the online version, at doi:10.1016/j.jphotochem.2009.07.029.

References

[1] B. O'Regan, M. Grätzel, Nature 353 (1991) 737–740.
[2] E. Stathatos, P. Lianos, Adv. Mater. 19 (2007) 3338–3341.
[3] A. Burke, S. Ito, H. Snaith, U. Bach, J. Kwiatkowski, M. Grätzel, Nano Lett. 8 (2008) 977–981.
[4] D.P. Hagberg, J.H. Yum, H. Lee, F. De Angelis, T. Marinado, K.M. Karlsson, R. Humphry-Baker, L. Sun, A. Hagfeldt, M. Grätzel, M.K. Nazeeruddin, J. Am. Chem. Soc. 130 (2008) 6259–6266.
[5] Q. Wang, Z. Zhang, S.M. Zakeeruddin, M. Grätzel, J. Phys. Chem. C 112 (2008) 7084–7092.
[6] Y. Kondo, H. Yoshikawa, K. Awaga, M. Murayama, T. Mori, K. Sunada, S. Bandow, S. Iijima, Langmuir 24 (2008) 547–550.
[7] M. Grätzel, J. Photochem. Photobiol. A: Chem. 164 (2004) 3–14.
[8] J. van de Lagemaat, A.J. Frank, J. Phys. Chem. B 105 (2001) 11194–11205.
[9] W. Zhou, K. Pan, L. Zhang, C. Tian, H. Fu, Phys. Chem. Chem. Phys. 11 (2009) 1713–1718.
[10] K. Zhu, T.B. Vinzant, N.R. Neale, A.J. Frank, Nano Lett. 7 (2007) 3739–3746.
[11] J. Tornow, K. Schwarzburg, J. Phys. Chem. C 111 (2007) 8692–8698.
[12] Y. Gao, M. Nagai, T.C. Chang, J.J. Shyue, Cryst. Growth Design 7 (2007) 2467–2471.
[13] J. Feng, A. Miedaner, P. Ahrenkiel, M.E. Himmel, C. Curtis, D. Ginley, J. Am. Chem. Soc. 127 (2005) 14968–14969.
[14] J.H. Lee, S.M. Yoon, K.K. Kim, I.S. Cha, Y.J. Park, J.Y. Choi, Y.H. Lee, U. Paik, J. Phys. Chem. C 112 (2008) 15267–15273.
[15] D. Lin, B. Xing, Environ. Sci. Technol. 42 (2008) 7254–7259.
[16] D. Simien, J.A. Fagan, W. Luo, J.F. Douglas, K. Migler, J. Obrzut, ACS Nano 2 (2008) 1879–1884.
[17] A. Kongkanand, R.M. Domínguez, P.V. Kamat, Nano Lett. 7 (2007) 676–680.
[18] J. Chen, M.J. Dyer, M.F. Yu, J. Am. Chem. Soc. 123 (2001) 6201–6202.
[19] K. Liu, M. Zhang, W. Zhou, L. Li, J. Wang, H. Fu, Nanotechnology 16 (2005) 3006–3011.
[20] L.Q. Jing, X.J. Sun, J. Shang, W.M. Cai, Z.L. Xu, Y.G. Du, H.G. Fu, Sol. Energy Mater. Sol. Cells 79 (2003) 133–151.
[21] P. Wang, L. Wang, B. Ma, B. Li, Y. Qiu, J. Phys. Chem. B 110 (2006) 14406–14409.
[22] J. Halme, G. Boschloo, A. Hagfeldt, P. Lund, J. Phys. Chem. C 112 (2008) 5623–5637.
[23] P.V. Kamat, K.G. Thomas, S. Barazzouk, G. Girishkumar, K. Vinodgopal, D. Meisel, J. Am. Chem. Soc. 126 (2004) 10757–10762.
[24] Y. Yang, L. Qu, L. Dai, T.S. Kang, M. Durstock, Adv. Mater. 19 (2007) 1239–1243.
[25] S. Osswald, E. Flahaut, Y. Gogotsi, Chem. Mater. 18 (2006) 1525–1533.
[26] P.V. Kamat, J. Phys. Chem. C 111 (2007) 2834–2860.
[27] G.K. Mor, K. Shankar, M. Paulose, O.K. Varghese, C.A. Grimes, Nano Lett. 6 (2006) 215–218.
[28] M. Law, L.E. Greene, J.C. Johnson, R. Saykally, P. Yang, Nat. Mater. 4 (2005) 455–459.
[29] V. Feigenbrugel, C. Loew, S.L. Calvé, P. Mirabel, J. Photochem. Photobiol. A: Chem. 174 (2005) 76–81.
[30] F. Lenzmann, K. Krueger, S. Burnside, K. Brooks, M. Grätzel, D. Gal, S. Rühle, D. Cahen, J. Phys. Chem. B 105 (2001) 6347–6352.
[31] P. Wang, D. Wang, H. Li, T. Xie, H. Wang, Z. Du, J. Colloid Interface Sci. 314 (2007) 337–340.
[32] L.Q. Jing, H.G. Fu, B.Q. Wang, D.J. Wang, B.F. Xin, S.D. Li, J.Z. Sun, Appl. Catal. B 62 (2006) 282–291.
[33] L. Kronik, Y. Shapira, Surf. Sci. Rep. 37 (1999) 1–206.
[34] L. Jing, S. Li, S. Song, L. Xue, H. Fu, Sol. Energy Mater. Sol. Cells 92 (2008) 1030–1036.
[35] A. Kongkanand, P.V. Kamat, ACS Nano 1 (2007) 13–21.
[36] P. Brown, K. Takechi, P.V. Kamat, J. Phys. Chem. C 112 (2008) 4776–4782.
[37] L.W. Zhang, H.B. Fu, Y.F. Zhu, Adv. Funct. Mater. 18 (2008) 2180–2189.
[38] B. Xin, Z. Ren, P. Wang, J. Liu, L. Jing, H. Fu, Appl. Surf. Sci. 253 (2007) 4390–4395.